

1   **Challenges and opportunities for porous media research to address PFAS groundwater**  
2   **contamination**

3   Bo Guo<sup>1,\*</sup> and Mark L. Brusseau<sup>1,2</sup>

4   <sup>1</sup>Department of Hydrology and Atmospheric Sciences, University of Arizona, USA

5   <sup>2</sup>Department of Environmental Science, University of Arizona, USA

6

7   Corresponding author: Bo Guo ([boguo@arizona.edu](mailto:boguo@arizona.edu))

8

9   **Abstract**

10   Per- and polyfluoroalkyl substances (PFAS) have become one of the most important  
11   contaminants due to their ubiquitous presence in the environment and potentially profound  
12   impacts on human health and the environment even at parts per trillion (ppt) concentration levels.  
13   A growing number of field investigations have revealed that soils serve as PFAS reservoirs at  
14   many contaminated sites after accumulating significant amounts of PFAS mass over many  
15   decades. Because PFAS accumulated in soils may migrate downward to contaminate  
16   groundwater resources, understanding the fate and transport of PFAS in soil is of paramount  
17   importance for characterizing, managing, and mitigating long-term groundwater contamination  
18   risks.

19   Many PFAS are surfactants that adsorb at air–water and solid–water interfaces, which leads  
20   to complex transport behaviors of PFAS in soils. Concomitantly, PFAS present in porewater can  
21   modify surface tension and other interfacial properties, which in turn may impact variably  
22   saturated flow and PFAS transport. Furthermore, some PFAS are volatile (i.e., can migrate in the  
23   gas phase) and/or can transform under environmental conditions into persistent PFAS. These  
24   nonlinear and coupled processes are further complicated by complexities of the soil environment  
25   such as thin water films, spatial heterogeneity, and complex geochemical conditions.

26   In this commentary, we present an overview of the current challenges in understanding the  
27   fate and transport of PFAS in the environment. Building upon that, we identify a few potential  
28   areas where porous media research may play an important role in addressing the problem of  
29   PFAS contamination in groundwater.

30 **Keywords:** Porous media, PFAS, fluid–fluid interfaces, fate and transport, soil, groundwater,  
31 adsorption

32

33 **1. The PFAS contamination problem**

34 PFAS is an acronym that stands for per- and polyfluoroalkyl substances, which are a family of  
35 thousands of synthetic chemicals widely used since the 1950s<sup>1</sup>. Large-scale manufacturing and  
36 applications (such as non-stick and stain-resistant coating, waterproofing treatment, and  
37 firefighting foams)<sup>1</sup> have led to their ubiquitous presence in the environment, contaminating  
38 surface water, soils, sediments, and groundwater. A growing body of field data demonstrates that  
39 vadose zones (below land surface and above groundwater table) at PFAS-contaminated sites  
40 have become significant PFAS reservoirs after accumulating mass over decades<sup>2</sup>, posing a long-  
41 term threat to groundwater resources underneath.

42 The problem of PFAS contamination is distinctive compared to most of the previous  
43 contaminants due to a combination of the following aspects. *First*, PFAS have been widely used  
44 for many industrial applications and consumer products over many decades. Long-term releases  
45 from various pathways and sources at different concentration levels (e.g., local concentrated  
46 sources of aqueous film forming (AFFF)-impacted sites vs. wider and much-less concentrated  
47 sources of agricultural lands receiving PFAS-containing biosolids) have resulted in their  
48 widespread presence in the environment. For example, at least 6,189 sites are known to be  
49 contaminated by PFAS in the United States<sup>3</sup> and 45% of the United States drinking water was  
50 estimated to contain PFAS<sup>4</sup>. Similarly, 22,934 contaminated sites have been reported across 32  
51 European countries with several countries (Belgium, Netherlands, Italy, Denmark, Germany,  
52 United Kingdom, and France) having more than 1,000 sites<sup>5,6</sup>. Note that these numbers may only  
53 reflect a fraction of the problem due to incomplete sampling and investigation. *Second*,  
54 unprecedentedly restrictive concentration levels have been established or are being discussed  
55 by regulatory agencies internationally. These concentration levels are several orders of magnitude  
56 lower than regulatory levels established for most prior contaminants<sup>7</sup>. For example, the maximum  
57 contaminant levels for PFOS and PFOA have been set to 4 parts per trillion (ppt) in the United  
58 States<sup>8</sup>. Even more restrictive regulations are used in some European countries such as  
59 Denmark<sup>9</sup> (i.e., 2 ppt for the sum of four PFAS). *Third*, PFAS consist of thousands of species with  
60 significantly different physicochemical properties (e.g., anionic vs. cationic vs. zwitterionic vs.  
61 neutral species, different functional groups, and carbon chain lengths) and transport behaviors.

62 *Fourth*, because vadose zones at many contaminated sites are PFAS reservoirs<sup>2</sup>, understanding  
63 and quantifying PFAS fate and transport in the vadose zone are central for characterizing,  
64 managing, and mitigating long-term groundwater contamination risks. The above-discussed  
65 characteristics lead to significant challenges to address the PFAS contamination problem.

66 Furthermore, most PFAS are surfactants that tend to accumulate at fluid–fluid and solid–fluid  
67 interfaces<sup>10</sup>. These interfacially-active properties lead to their relatively unique transport behaviors  
68 in the environment, particularly in the vadose zone due to abundant air–water and solid–water  
69 interfaces in soils. Concomitantly, PFAS accumulating at fluid–fluid and solid–fluid interfaces can  
70 also modify the properties of the interfaces<sup>10</sup>, including surface tension and wettability. The  
71 changes in interfacial properties may in turn impact variably saturated water flow and the transport  
72 of PFAS in the vadose zone<sup>11,12</sup>. Any effective characterization and remediation of contaminated  
73 vadose zones will require conceptualizations that incorporate these critical interfacial processes.  
74 In this commentary, we focus on discussing these complexities of PFAS fate and transport in the  
75 vadose zone and identify the challenges and opportunities where porous media research may be  
76 relevant.

77 **2. Complexity of the PFAS problem from a fate and transport perspective.**

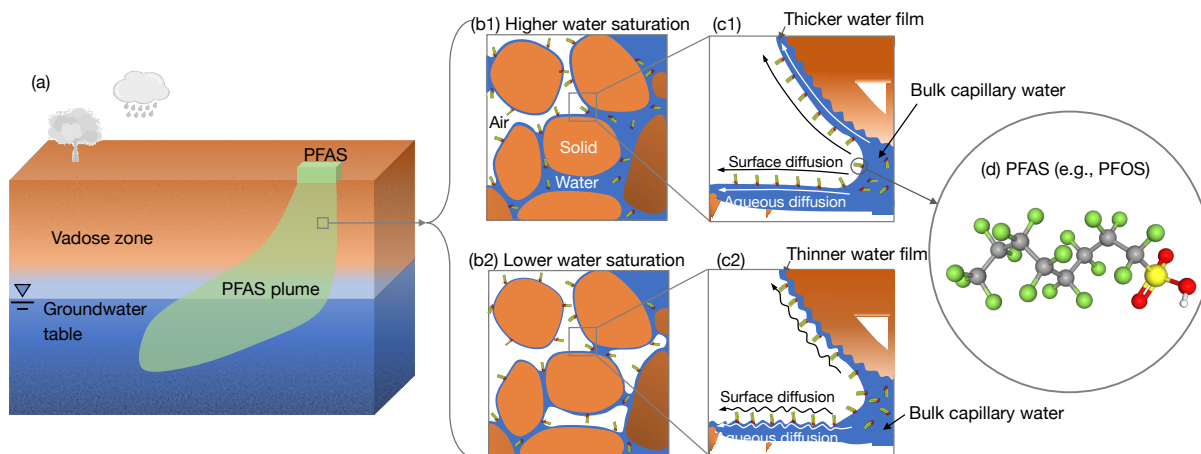


**Figure 1.** Interfacial retention processes for PFAS in the vadose zone. (a) Schematic for PFAS contamination in the vadose zone and groundwater, (b) adsorption of PFAS at air–water interfaces arising from bulk capillary water and thin water films in soils under different wetting conditions, (c) mass transfer of PFAS between bulk capillary water and thin water films, and (d) an example PFAS molecule (e.g., PFOS), where the colors denote different atoms: gray–carbon, green–fluorine, red–oxygen, yellow–sulfur, and white–hydrogen. In panel (d), the molecule consists of a hydrophobic and oleophobic tail (the fluorocarbon chain on the left) and a hydrophilic head (the sulfonic acid functional group on the right). Figure originally reported in Chen & Guo (2023)<sup>65</sup> and used here with permission of the authors and Wiley.

78 Air–water interfaces in the vadose zone may arise from the bulk water (e.g., pendular rings)  
79 between soil grains (i.e., bulk capillary air–water interfaces) and the thin water films on grain  
80 surfaces (Fig. 1). Under most field-relevant conditions, the latter accounts for >90% of air–water  
81 interfaces<sup>13–18</sup>. Air–water interfacial adsorption has been demonstrated to be a major mechanism  
82 controlling the fate and transport of PFAS in the vadose zone by laboratory column transport  
83 experiments<sup>19–24</sup>, field observations<sup>25,26</sup>, and mathematical modeling<sup>11,12,27–32</sup>. These studies  
84 highlight the importance of understanding and quantifying partitioning of PFAS at air–water  
85 interfaces in soils and how it controls PFAS transport in the vadose zone.

86 Fluid–fluid interfaces have been long recognized as an important factor controlling flow,  
87 transport, and reactions in porous media<sup>33</sup>. The processes at fluid–fluid interfaces include  
88 adsorption and desorption of interfacially-active solutes<sup>34–38</sup>, attachment and detachment of  
89 colloids<sup>39–42</sup>, and mass transfer between fluid phases<sup>43,44</sup>. One of the earlier drivers to quantify  
90 air–water interfacial area was to test a functional relationship among capillary pressure, saturation,  
91 and fluid–fluid interfacial area in a porous medium derived from thermodynamic principles<sup>45–47</sup>. A  
92 corollary of this functional relationship suggests that accounting for air–water interfacial area may  
93 eliminate hysteretic behaviors observed in capillary pressure and saturation relationships during  
94 cyclic drainage and imbibition processes<sup>45–48</sup>. Driven by this fundamental investigation and other  
95 more applied problems (e.g., dissolution of non-aqueous phase liquids [NAPL] in groundwater),  
96 multiple experimental methods have been developed to measure fluid–fluid interfacial areas in  
97 porous media since the late 1990s. One group of methods uses pore-scale imaging to explicitly  
98 count interfacial areas, such as X-ray computed tomography (XMT)<sup>49–55</sup>. Another group uses  
99 interfacially-active tracers to indirectly measure and compute fluid–fluid interfaces, either by  
100 retardation in the breakthrough curves during transport experiments or the mass of a tracer at  
101 fluid–fluid interfaces<sup>34,35,37,56–59</sup>. These interfacially-active tracers can be in the gas or liquid phase.  
102 Usually, the gas-phase tracer is an alkane (i.e., not charged) and the liquid-phase tracer an  
103 anionic hydrocarbon surfactant (i.e., negatively charged). Additionally, air–water interfacial area  
104 can also be estimated from measured soil water characteristic curves using a thermodynamic  
105 approach based on energy balance<sup>60,61</sup>.

106 XMT (and other imaging-based methods) can separate thin-film fluid–fluid interfaces from bulk  
 107 capillary interfaces. For a water saturation smaller than 0.5, the former measured by XMT is  
 108 generally much greater than the latter in natural porous media<sup>54,55</sup>. The actual thin-film fluid–fluid  
 109 interfacial area is usually even much greater because XMT underestimates the thin-film fluid–fluid  
 110 interfacial area for sand and soil media. The cause is XMT not measuring the additional thin-film  
 111 interfacial area due to the microscale grain surface roughness<sup>13,55</sup>. For example, by combining  
 112 XMT and liquid-phase tracer methods, Brusseau et al. (2007)<sup>13</sup> reported that thin-film fluid–fluid  
 113 interfacial areas in a sandy soil accounted for >90% of the total fluid–fluid interfacial area at water  
 114 saturations smaller than 0.5. Further, the fluid–fluid interfacial area measured by gas-phase tracer  
 115 methods is greater than that by liquid-phase tracers, especially under drier conditions<sup>13,18,62</sup>. The  
 116 significant difference between the fluid–fluid interfacial area measured by liquid- versus gas-  
 117 phase tracers remains not fully understood, though it was hypothesized that gas-phase tracers  
 118 may access additional air–water interfacial domains<sup>18,63</sup>. An example of the differences between  
 119 the air–water interfacial areas determined by the different methods is presented in Fig. 2<sup>63</sup>.

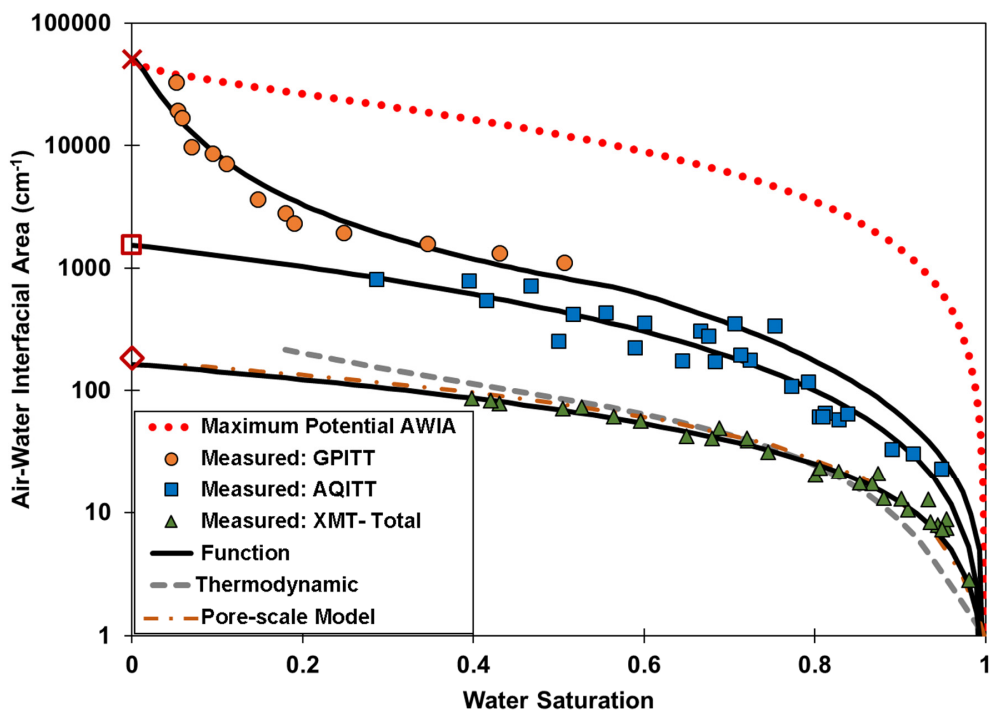


**Figure 2.** Air–water interfacial area as a function of water saturation for a sand determined by different measurement methods and models. “GPITT” denotes gas-phase interfacial tracer test, “AQITT” denotes aqueous interfacial tracer test. “XMT-total” is the total air–water interfacial area (bulk capillary and film-associated air–water interfacial area) measured by XMT. “Function” refers to an empirical fit. “Thermodynamic” denotes the results computed from the thermodynamic approach<sup>60,61</sup>. “Pore-scale Model” refers to the air–water interfacial area computed by the model from Jiang et al (2020)<sup>17</sup>. Figure originally reported in Brusseau (2023)<sup>63</sup> and used here with permission of the author and Elsevier.

120 While the prior works quantifying the air–water interfacial area made the distinction between  
121 the bulk capillary and thin-water-film air–water interfaces, the two types of air–water interfaces  
122 are not differentiated in most transport model conceptualizations for the retention and transport  
123 of interfacially-active contaminants. These model concepts often build upon two premises that  
124 significantly underrepresent the role of thin water films: 1) adsorption at the bulk capillary and thin-  
125 film air–water interfaces can be treated the same; and 2) interfacially-active contaminants in the  
126 thin water films and the bulk capillary water are in chemical equilibrium. These assumptions may  
127 be challenged in the vadose zone, especially under drier conditions. Recent theoretical analysis<sup>64</sup>  
128 illustrated that the adsorption of PFAS at thin-film air–water interfaces can strongly deviate from  
129 that at a bulk capillary air–water interface due to complex surface forces from the solid surface  
130 (i.e., electrostatic and Van der Waals forces). Additionally, slow mass transfer in thin water films  
131 can greatly reduce the accessibility of thin-film air–water interfaces for PFAS, and thereby  
132 introduce nonequilibrium conditions between thin water films and bulk capillary water<sup>65</sup> (Fig. 1).  
133 Surface diffusion of the adsorbed PFAS along air–water interfaces, while rarely discussed in the  
134 hydrology and PFAS literature, was identified as a primary mechanism for transferring PFAS mass  
135 along the thin water films and between the thin water films and bulk water<sup>65</sup>. The potentially slow  
136 mass transfer along the thin water films may also provide a plausible explanation for some of the  
137 differences observed between the air–water interfacial areas measured by liquid- and gas-tracer  
138 methods. Because thin water films account for most air–water interfaces in the vadose zone, not  
139 representing the above thin-film-mediated fundamental processes may predict significantly  
140 different field-scale migration of PFAS.

141 It is important to point out that the impact of air–water interfaces has been studied previously  
142 for the transport of interfacially-active constituents before PFAS, such as the attachment and  
143 detachment of colloidal particles at air–water interfaces<sup>66–69</sup>. The impact of water films on colloidal  
144 transport was also examined, but the modeled mechanisms are simple—films trap and immobilize  
145 colloids with a diameter greater than their thickness<sup>41,69</sup>—without representing any of the complex  
146 surface forces. Additionally, non-PFAS surfactants in the subsurface were also studied for various  
147 applications including enhanced oil recovery<sup>70,71</sup>, surfactant-enhanced aquifer remediation<sup>72,73</sup>,  
148 and the impact of surfactant on unsaturated water flow<sup>38,74–76</sup>. Somewhat surprisingly, all the  
149 earlier surfactant-related work primarily focused on how surfactants affect fluid flow and  
150 dissolution with minimal discussion of air–water interfacial adsorption (see more detailed  
151 discussion in Guo et al. (2020)<sup>11</sup>). In contrast, the impact of air–water interfacial adsorption on  
152 transport has been a focal point of the recent PFAS work.

153 In addition to the different interfacial area domains and thin water films, PFAS transport in the  
154 vadose zone involves several other complexities. *First*, PFAS interfacial partitioning is sensitive  
155 to geochemical conditions (e.g., water chemistry and interactions with other interfacially-active  
156 constituents). For example, the partitioning of PFAS at air–water interfaces can vary greatly under  
157 different ionic strengths and electrolyte compositions<sup>20,64,77–82</sup>. The presence of co-PFAS and other  
158 interfacially-active solutes may also modify the strength of air–water interfacial partitioning<sup>80,81,83,84</sup>.  
159 *Second*, in addition to accumulating at air–water interfaces, it was also hypothesized that PFAS  
160 may form supramolecular structures<sup>85</sup> such as aggregated structures, micelles, and vesicles.  
161 While micelles and vesicles are unlikely to be present due to porewater concentrations at PFAS-  
162 contaminated sites being much smaller than the critical micelle concentrations<sup>26,81</sup>, self-  
163 assemblies of *different* PFAS molecules may still arise in complex PFAS mixtures. If present, the  
164 movement of these supramolecular structures can transport PFAS themselves as well as  
165 partitioning mass with the other phases (aqueous phase, air–water interfaces, and solid surfaces).  
166 *Third*, strong transient flow dynamics coupled with spatial heterogeneity may introduce transport  
167 behaviors unique to PFAS due to partitioning to air–water interfaces and mass redistribution  
168 among the different phases. An example is the amplified acceleration of PFAS transport along  
169 preferential flow pathways with reduced air–water interfacial retention due to greater water  
170 saturation collapsing air-water interfaces<sup>12,31</sup>.

171 Finally, while most of the current PFAS fate and transport work focuses on anionic PFAS (i.e.,  
172 perfluoroalkyl acids, [PFAAs]), other types of PFAS including cationic, zwitterionic, and neutral  
173 compounds have been shown to be present at contaminated sites<sup>86–92</sup>. Unlike the environmentally  
174 persistent PFAAs, some of these PFAS can react under environmental conditions—driven by  
175 either abiotic or biotic processes—and eventually transform into PFAAs<sup>93–95</sup>. The fate and  
176 transport of these PFAA “precursors” in the vadose zone remain poorly understood. Furthermore,  
177 some of the neutral PFAS have relatively high vapor pressure and may partition to the gas phase  
178 as PFAS vapor<sup>96,97</sup>. The migration of vapor-phase PFAS and their partitioning with the other  
179 phases represent another set of potentially important processes for PFAS transport in the vadose  
180 zone<sup>96</sup>.

### 181 **3. Challenges and opportunities for porous media research**

182 While great progress has been made over the past few years that advances our understanding  
183 of the fate and transport of PFAS in the vadose zone, many important areas are under explored  
184 and significant challenges remain. Here we comment on some of the major challenges from the  
185 perspectives of both fundamental research and practical applications.

186 • *Quantification of air-water interfacial area.* Various methods including direct imaging-based  
187 and indirect tracer-based approaches were developed to measure or estimate air–water  
188 interfacial area at varying water saturations as discussed in Section 2. However, there are still  
189 internal inconsistencies among these different methods, e.g., different methods may measure  
190 different air–water interfacial areas under the same conditions for the same media.  
191 Furthermore, the characterization of air–water interfacial area has only been done on a very  
192 limited number of soils. Because air–water interfaces play a primary role in controlling the  
193 transport of interfacially-active substances such as PFAS, it is important to conduct  
194 comprehensive investigations of air–water interfacial area for a variety of soils and under  
195 different wetting conditions, as discussed recently<sup>63</sup>. These detailed characterizations may  
196 then allow for the development of process-based models or robust empirical correlations for  
197 the air–water interfacial area as functions of other more readily available parameters. These  
198 improved quantifications of air–water interfacial area are expected to significantly advance the  
199 modeling of PFAS fate and transport in the vadose zone.

200 • *Coupled nonlinear multi-physics processes.* The transport of PFAS is a multi-physics problem  
201 that involves various nonlinear processes in the vadose zone. For example, while surfactant-  
202 induced flow may not be significant for many lower concentration sites<sup>11,12</sup>, they could modify  
203 the transport behavior of PFAS at some of the highly contaminated AFFF-impacted sites<sup>11,12,98</sup>,  
204 especially in the early period of PFAS release from fire training activities. Additionally, PFAS  
205 are almost always present at contaminated sites as mixtures of a large variety of individual  
206 PFAS and other substances. A few initial experiment studies have examined the impact of  
207 PFAS mixtures and hydrocarbon surfactants on the interfacial tension<sup>77,99–102</sup> and  
208 transport<sup>84,103–106</sup>. The multicomponent Langmuir model was used to describe potential  
209 competitive adsorption among different components<sup>80,84,105–107</sup>, but the multicomponent  
210 Langmuir model has been argued to be thermodynamically inconsistent unless all  
211 components have equal maximum adsorption capacity<sup>81,108–111</sup>. A more rigorous  
212 thermodynamically consistent model was recently developed for multicomponent adsorption  
213 of PFAS<sup>81</sup>. However, all the studies to date focus primarily on PFAS mixtures with no opposite  
214 charges. The potentially synergistic interactions among PFAS with opposite charges (e.g.,  
215 between anionic and cationic PFAS) and how they affect the fate and transport of PFAS in the  
216 vadose zone remain minimally explored. The same goes to the transport of PFAS in the vapor  
217 phase and the transformation of PFAA precursors. On top of the processes discussed above,  
218 PFAS transport in the vadose zone is also driven by transient and nonlinear variably saturated  
219 flow, which has been considered as one of the most computationally challenging processes

220 in hydrology<sup>112,113</sup>. Understanding and quantifying how all these processes and their coupling  
221 control PFAS transport in the vadose zone will require comprehensive experimental and field  
222 data, as well as development of new mathematical models and numerical methods.

223 • *Physical chemistry of PFAS interfacial partitioning and mass transfer in the thin water films,  
224 and how they manifest at greater spatial scales.* While the importance of thin water films has  
225 been recognized in porous media literature for fluid displacement, they are often considered  
226 insignificant for solute transport because they represent a tiny fraction of the total fluid volume  
227 and hence a negligible amount of the solute mass. This conceptualization needs to be revised  
228 for PFAS transport because the majority of the PFAS mass may be associated with the thin  
229 water films due to the significant amounts of air–water interfaces arising from the thin water  
230 films. Whether these thin water films can be accessed by PFAS, and under what conditions  
231 they occur, may directly affect PFAS transport in the vadose zone<sup>31,65</sup>. Furthermore, the  
232 physical chemistry of PFAS partitioning at the air–water interface in the vicinity of a complex  
233 solid surface may deviate from that at bulk air–water interfaces<sup>64</sup>. These detailed processes  
234 occurring in the thin water films are potentially critical but are only begun to be explored.

235 • *Scale translation and the development of practical modelling approaches.* An outstanding  
236 challenge prevalent in all subsurface-related problems is the significant disparity between the  
237 scales at which dominant physical and chemical processes occur (nanometers to millimeters)  
238 and that at which we make observations and engineering decisions (tens of centimeters to  
239 meters or larger). This is also the case for PFAS transport in the vadose zone. Ultimately, site  
240 characterization and remediation applications need models developed for the field scale that  
241 can be practically applied to real-world contaminated sites. These practical models must be  
242 computationally efficient and relatively simple to parameterize, which means that they likely  
243 cannot account for all the complexities discussed in Section 2. We will need to identify the  
244 sub-pore and pore-scale processes with a first-order impact and approximate them at  
245 macroscales. Experimental data and more advanced models that represent a greater level of  
246 complexities may be used to aid the development of these practical models<sup>65</sup>.

247 We point out that the aspects discussed above are by no means an exhaustive list of important  
248 topics for PFAS transport in the vadose zone. Rather, they represent a sample of the topics that  
249 we think the porous media community may find interesting. Addressing each of these challenges  
250 will likely require an integrated investigation through experiments, field observations, and  
251 development of theory and computational models from sub-pore-scale, pore-scale, and  
252 macroscales. Just like the prior non-PFAS research efforts that helped to prepare us for tackling

253 the PFAS contamination problem, the fate and transport research of PFAS will likely generate  
254 new knowledge and tools that may find use in addressing emerging environmental problems in  
255 the future, with the interfacially-active micro- and nano-plastics being a potential example.

256 **4. Conclusion**

257 This commentary provides an overview of the complexities and challenges for understanding and  
258 quantifying the fate and transport of PFAS in the environment, with a particular focus on the  
259 vadose zone. We have centered on issues unique to PFAS relative to many of the previous  
260 contaminants, and how these processes manifest in the complex porous media environment. It  
261 has become clear that the PFAS contamination problem is one that can significantly benefit from  
262 the expertise of the porous media community both from fundamental and practical perspectives.  
263 This commentary is an attempt to highlight some of the opportunities to which the porous media  
264 community may make significant contributions.

265 **5. Acknowledgment**

266 This work was in part supported by National Science Foundation CAREER Award (2237015) to  
267 B. Guo and by the Environmental Security Technology Certification Program (ESTCP Project  
268 ER21-5041) to B. Guo and M. L. Brusseau.

269 **6. References**

270 (1) ITRC. *ITRC PFAS Technical and Regulatory Guidance Document*; 2024.

271 (2) Brusseau, M. L.; Anderson, R. H.; Guo, B. PFAS Concentrations in Soils: Background  
272 Levels versus Contaminated Sites. *Science of the Total Environment* **2020**, *740*,  
273 140017. <https://doi.org/10.1016/j.scitotenv.2020.140017>.

274 (3) EWG. *PFAS Contamination in the U.S.*; 2024. [https://www.ewg.org/interactive-maps/pfas\\_contamination/](https://www.ewg.org/interactive-maps/pfas_contamination/) (accessed 2024-08-04).

275 (4) Smalling, K. L.; Romanok, K. M.; Bradley, P. M.; Morriss, M. C.; Gray, J. L.; Kanagy, L.  
276 K.; Gordon, S. E.; Williams, B. M.; Breitmeyer, S. E.; Jones, D. K.; DeCicco, L. A.;  
277 Eagles-Smith, C. A.; Wagner, T. Per- and Polyfluoroalkyl Substances (PFAS) in United  
278 States Tapwater: Comparison of Underserved Private-Well and Public-Supply  
279 Exposures and Associated Health Implications. *Environ Int* **2023**, *178*, 108033.  
280 <https://doi.org/10.1016/j.envint.2023.108033>.

281 (5) Cordner, A.; Brown, P.; Cousins, I. T.; Scheringer, M.; Martinon, L.; Dagorn, G.; Aubert,  
282 R.; Hosea, L.; Salvidge, R.; Felke, C.; Tausche, N.; Drepper, D.; Liva, G.; Tudela, A.;

284 Delgado, A.; Salvatore, D.; Pilz, S.; Horel, S. PFAS Contamination in Europe:  
285 Generating Knowledge and Mapping Known and Likely Contamination with “Expert-  
286 Reviewed” Journalism. *Environ Sci Technol* **2024**, *58* (15), 6616–6627.  
287 <https://doi.org/10.1021/acs.est.3c09746>.

288 (6) The Forever Pollution Project. *The Forever Pollution Project: Journalists tracking PFAS*  
289 *across Europe*. <https://foreverpollution.eu/> (accessed 2024-07-08).

290 (7) Newell, C. J.; Adamson, D. T.; Kulkarni, P. R.; Nzeribe, B. N.; Stroo, H. Comparing  
291 PFAS to Other Groundwater Contaminants : Implications for Remediation. **2020**, 7–  
292 26. <https://doi.org/10.1002/rem.21645>.

293 (8) US EPA. *Final PFAS National Primary Drinking Water Regulation*.  
294 <https://www.epa.gov/sdwa/and-polyfluoroalkyl-substances-pfas> (accessed 2024-  
295 08-04).

296 (9) Danish EPA. *Limit values for PFAS in the environment*. <https://mst.dk/erhverv/sikker->  
297 [kemi/kemikalier/graensevaerdier-og-kvalitetskriterier](https://mst.dk/erhverv/sikker-kemi/kemikalier/graensevaerdier-og-kvalitetskriterier) (accessed 2024-08-04).

298 (10) Kiss, E. *Fluorinated Surfactants and Repellents*, Second.; CRC Press, 2001; Vol. 97.

299 (11) Guo, B.; Zeng, J.; Brusseau, M. L. A Mathematical Model for the Release, Transport,  
300 and Retention of Per- and Polyfluoroalkyl Substances (PFAS) in the Vadose Zone.  
301 *Water Resour Res* **2020**, *56* (2), 1–21. <https://doi.org/10.1029/2019WR026667>.

302 (12) Zeng, J.; Guo, B. Multidimensional Simulation of PFAS Transport and Leaching in the  
303 Vadose Zone: Impact of Surfactant-Induced Flow and Subsurface Heterogeneities.  
304 *Adv Water Resour* **2021**, *155*, 104015.  
305 <https://doi.org/10.1016/j.advwatres.2021.104015>.

306 (13) Brusseau, M. L.; Peng, S.; Schnaar, G.; Murao, A. Measuring Air-Water Interfacial  
307 Areas with X-Ray Microtomography and Interfacial Partitioning Tracer Tests. *Environ*  
308 *Sci Technol* **2007**, *41* (6), 1956–1961. <https://doi.org/10.1021/es061474m>.

309 (14) Brusseau, M. L.; Peng, S.; Schnaar, G.; Costanza-Robinson, M. S. Relationships  
310 among Air-Water Interfacial Area, Capillary Pressure, and Water Saturation for a  
311 Sandy Porous Medium. *Water Resour Res* **2006**, *42* (3), 1–5.  
312 <https://doi.org/10.1029/2005WR004058>.

313 (15) Kibbey, T. C. G.; Chen, L. A Pore Network Model Study of the Fluid-Fluid Interfacial  
314 Areas Measured by Dynamic-Interface Tracer Depletion and Miscible Displacement  
315 Water Phase Advective Tracer Methods. *Water Resour Res* **2012**, *48* (10).  
316 <https://doi.org/10.1029/2012WR011862>.

317 (16) Or, D.; Tuller, M. Liquid Retention and Interfacial Area in Variably Saturated Porous  
318 Media: Upscaling from Single-Pore to Sample-Scale Model. *Water Resour Res* **1999**,  
319 35 (12), 3591–3605.

320 (17) Jiang, H.; Guo, B.; Brusseau, M. L. Pore-Scale Modeling of Fluid-Fluid Interfacial Area  
321 in Variably Saturated Porous Media Containing Microscale Surface Roughness. *Water*  
322 *Resour Res* **2020**, 56 (1), 1–21. <https://doi.org/10.1029/2019WR025876>.

323 (18) Costanza-Robinson, M. S.; Brusseau, M. L. Air-Water Interfacial Areas in Unsaturated  
324 Soils: Evaluation of Interfacial Domains. *Water Resour Res* **2002**, 38 (10), 13-1-13-17.  
325 <https://doi.org/10.1029/2001wr000738>.

326 (19) Lyu, Y.; Brusseau, M. L.; Chen, W.; Yan, N.; Fu, X.; Lin, X. Adsorption of PFOA at the  
327 Air-Water Interface during Transport in Unsaturated Porous Media. *Environ Sci*  
328 *Technol* **2018**, 52 (14), 7745–7753. <https://doi.org/10.1021/acs.est.8b02348>.

329 (20) Brusseau, M. L.; Van Glubt, S. The Influence of Molecular Structure on PFAS  
330 Adsorption at Air-Water Interfaces in Electrolyte Solutions. *Chemosphere* **2021**, 281  
331 (May), 130829. <https://doi.org/10.1016/j.chemosphere.2021.130829>.

332 (21) Brusseau, M. L.; Guo, B.; Huang, D.; Yan, N.; Lyu, Y. Ideal versus Nonideal Transport  
333 of PFAS in Unsaturated Porous Media. *Water Res* **2021**, 202, 117405.  
334 <https://doi.org/10.1016/j.watres.2021.117405>.

335 (22) Stults, J. F.; Choi, Y. J.; Schaefer, C. E.; Illangasekare, T. H.; Higgins, C. P. Estimation of  
336 Transport Parameters of Perfluoroalkyl Acids (PFAAs) in Unsaturated Porous Media:  
337 Critical Experimental and Modeling Improvements. *Environ Sci Technol* **2022**, 56  
338 (12), 7963–7975. <https://doi.org/10.1021/acs.est.2c00819>.

339 (23) Lyu, X.; Liu, X.; Sun, Y.; Gao, B.; Ji, R.; Wu, J.; Xue, Y. Importance of Surface  
340 Roughness on Perfluorooctanoic Acid (PFOA) Transport in Unsaturated Porous  
341 Media. *Environmental Pollution* **2020**, 266, 115343.  
342 <https://doi.org/10.1016/j.envpol.2020.115343>.

343 (24) Bigler, M.; He, X.; Brusseau, M. L. PFAS Transport under Lower Water-Saturation  
344 Conditions Characterized with Instrumented-Column Systems. *Water Res* **2024**,  
345 260, 121922. <https://doi.org/10.1016/j.watres.2024.121922>.

346 (25) Schaefer, C. E.; Lavorgna, G. M.; Lippincott, D. R.; Nguyen, D.; Christie, E.; Shea, S.;  
347 O'Hare, S.; Lemes, M. C. S.; Higgins, C. P.; Field, J. A Field Study to Assess the Role of  
348 Air-Water Interfacial Sorption on PFAS Leaching in an AFFF Source Area. *J Contam*  
349 *Hydrol* **2022**, 248 (July 2021), 104001.  
350 <https://doi.org/10.1016/j.jconhyd.2022.104001>.

351 (26) Brusseau, M. L.; Guo, B. PFAS Concentrations in Soil versus Soil Porewater: Mass  
352 Distributions and the Impact of Adsorption at Air-Water Interfaces. *Chemosphere*  
353 **2022**, 302, 134938. <https://doi.org/10.1016/j.chemosphere.2022.134938>.

354 (27) Zeng, J.; Brusseau, M. L.; Guo, B. Model Validation and Analyses of Parameter  
355 Sensitivity and Uncertainty for Modeling Long-Term Retention and Leaching of PFAS  
356 in the Vadose Zone. *J Hydrol (Amst)* **2021**, 127172.  
357 <https://doi.org/10.1016/j.jhydrol.2021.127172>.

358 (28) Gnesda, W. R.; Draxler, E. F.; Tinjum, J.; Zahasky, C. Adsorption of PFAAs in the  
359 Vadose Zone and Implications for Long-Term Groundwater Contamination. *Environ  
360 Sci Technol* **2022**, 56 (23), 16748–16758. <https://doi.org/10.1021/acs.est.2c03962>.

361 (29) Wallis, I.; Hutson, J.; Davis, G.; Kookana, R.; Rayner, J.; Prommer, H. Model-Based  
362 Identification of Vadose Zone Controls on PFAS Mobility under Semi-Arid Climate  
363 Conditions. *Water Res* **2022**, 225 (May), 119096.  
364 <https://doi.org/10.1016/j.watres.2022.119096>.

365 (30) Silva, J. A. K.; Šimůnek, J.; McCray, J. A Modified HYDRUS Model for Simulating PFAS  
366 Transport in the Vadose Zone. *Water (Basel)* **2020**, 12 (10), 2758.  
367 <https://doi.org/10.3390/w12102758>.

368 (31) Zeng, J.; Guo, B. Reduced Accessible Air–Water Interfacial Area Accelerates PFAS  
369 Leaching in Heterogeneous Vadose Zones. *Geophys Res Lett* **2023**, 50 (8), 1–10.  
370 <https://doi.org/10.1029/2022GL102655>.

371 (32) Guo, B.; Zeng, J.; Brusseau, M. L.; Zhang, Y. A Screening Model for Quantifying PFAS  
372 Leaching in the Vadose Zone and Mass Discharge to Groundwater. *Adv Water Resour*  
373 **2022**, 160 (104102). <https://doi.org/10.1016/j.advwatres.2021.104102>.

374 (33) Bear, J. *Dynamics of Fluids in Porous Media*; Elsevier: New York, 1972.

375 (34) Kim, H.; Rao, P. S. C.; Annable, D. Determination of Effective Air-Water Interfacial  
376 Area in Partially Saturated Porous Media Using Surfactant Adsorption. *Water Resour  
377 Res* **1997**, 33 (12), 2705–2711.

378 (35) Saripalli, K. P.; Kim, H.; Rao, P. S. C.; Annable, M. D. Measurement of Specific Fluid-  
379 Fluid Interfacial Areas of Immiscible Fluids in Porous Media. *Environ Sci Technol*  
380 **1997**, 31 (3), 932–936. <https://doi.org/10.1021/es960652g>.

381 (36) Karkare, M. V.; Fort, T. Determination of the Air-Water Interfacial Area in Wet  
382 “Unsaturated” Porous Media. *Langmuir* **1996**, 12 (8), 2041–2044.  
383 <https://doi.org/10.1021/la950821v>.

384 (37) Faisal Anwar, A. H. M.; Bettahar, M.; Matsubayashi, U. A Method for Determining Air-  
385 Water Interfacial Area in Variably Saturated Porous Media. *J Contam Hydrol* **2000**, *43*  
386 (2), 129–146. [https://doi.org/10.1016/S0169-7722\(99\)00103-5](https://doi.org/10.1016/S0169-7722(99)00103-5).

387 (38) Smith, J. E.; Gillham, R. W. Effects of Solute Concentration-Dependent Surface  
388 Tension on Unsaturated Flow: Laboratory Sand Column Experiments. *Water Resour  
389 Res* **1999**, *35* (4), 973–982. <https://doi.org/10.1029/1998WR900106>.

390 (39) Lenhart, J. J.; Saiers, J. E. Adsorption of Natural Organic Matter to Air-Water Interfaces  
391 during Transport through Unsaturated Porous Media. *Environ Sci Technol* **2004**, *38*  
392 (1), 120–126. <https://doi.org/10.1021/es034409a>.

393 (40) Gao, B.; Saiers, J. E.; Ryan, J. N. Deposition and Mobilization of Clay Colloids in  
394 Unsaturated Porous Media. *Water Resour Res* **2004**, *40* (8), 1–8.  
395 <https://doi.org/10.1029/2004WR003189>.

396 (41) Wan, J.; Tokunaga, T. K. Film Straining of Colloids in Unsaturated Porous Media:  
397 Conceptual Model and Experimental Testing. *Environ Sci Technol* **1997**, *31* (8), 2413–  
398 2420. <https://doi.org/10.1021/es970017q>.

399 (42) Torkzaban, S.; Hassanizadeh, S. M.; Schijven, J. F.; Van Den Berg, H. H. J. L. Role of  
400 Air-Water Interfaces on Retention of Viruses under Unsaturated Conditions. *Water  
401 Resour Res* **2006**, *42* (12), 1–11. <https://doi.org/10.1029/2006WR004904>.

402 (43) Miller, C. T.; Poirier-McNeil, M. M.; Mayer, A. S. Dissolution of Trapped Nonaqueous  
403 Phase Liquids: Mass Transfer Characteristics. *Water Resour Res* **1990**, *26* (11), 2783–  
404 2796. <https://doi.org/10.1029/WR026i011p02783>.

405 (44) Powers, S. E.; Loureiro, C. O.; Abriola, L. M.; Weber, W. J. Theoretical Study of the  
406 Significance of Nonequilibrium Dissolution of Nonaqueous Phase Liquids in  
407 Subsurface Systems. *Water Resour Res* **1991**, *27* (4), 463–477.  
408 <https://doi.org/10.1029/91WR00074>.

409 (45) Hassanizadeh, S. M.; Gray, W. G. Mechanics and Thermodynamics of Multiphase  
410 Flow in Porous Media Including Interphase Boundaries. *Adv Water Resour* **1990**, *13*  
411 (4), 169–186. [https://doi.org/10.1016/0309-1708\(90\)90040-B](https://doi.org/10.1016/0309-1708(90)90040-B).

412 (46) Hassanizadeh, S. M.; Gray, W. G. Thermodynamic Basis of Capillary Pressure in  
413 Porous Media. *Water Resour Res* **1993**, *29* (10), 3389–3405.  
414 <https://doi.org/10.1029/93WR01495>.

415 (47) Hassanzadeh, M. S.; Gray, W. G. Toward an Improved Description of the Physics of  
416 Two-Phase Flow. *Adv Water Resour* **1993**, *16* (1), 53–67.  
417 [https://doi.org/10.1016/0309-1708\(93\)90029-F](https://doi.org/10.1016/0309-1708(93)90029-F).

418 (48) Reeves, P. C.; Celia, M. a. A Functional-Relationship between Capillary-Pressure,  
419 Saturation, and Interfacial Area as Revealed by a Pore-Scale Network Model. *Water*  
420 *Resour Res* **1996**, *32* (8), 2345–2358. <https://doi.org/10.1029/96WR01105>.

421 (49) Culligan, K. A.; Wildenschild, D.; Christensen, B. S. B.; Gray, W. G.; Rivers, M. L.;  
422 Tompson, A. F. B. Interfacial Area Measurements for Unsaturated Flow through a  
423 Porous Medium. *Water Resour Res* **2004**, *40* (12), 1–12.  
424 <https://doi.org/10.1029/2004WR003278>.

425 (50) Schnaar, G.; Brusseau, M. L. Pore-Scale Characterization of Organic Immiscible-  
426 Liquid Morphology in Natural Porous Media Using Synchrotron x-Ray  
427 Microtomography. *Environ Sci Technol* **2005**, *39* (21), 8403–8410.  
428 <https://doi.org/10.1021/es0508370>.

429 (51) Wildenschild, D.; Sheppard, A. P. X-Ray Imaging and Analysis Techniques for  
430 Quantifying Pore-Scale Structure and Processes in Subsurface Porous Medium  
431 Systems. *Adv Water Resour* **2013**, *51*, 217–246.  
432 <https://doi.org/10.1016/j.advwatres.2012.07.018>.

433 (52) Wildenschild, D.; Rivers, M. L.; Porter, M. L.; Iltis, G. C.; Armstrong, R. T.; Davit, Y.  
434 Using Synchrotron-Based X-Ray Microtomography and Functional Contrast Agents in  
435 Environmental Applications. **2015**, 1–22. <https://doi.org/10.2136/sssaspecpub61.c1>.

436 (53) Culligan, K. A.; Wildenschild, D.; Christensen, B. S. B.; Gray, W. G.; Rivers, M. L. Pore-  
437 Scale Characteristics of Multiphase Flow in Porous Media: A Comparison of Air-  
438 Water and Oil–Water Experiments. *Adv Water Resour* **2006**, *29* (2), 227–238.  
439 <https://doi.org/10.1016/j.advwatres.2005.03.021>.

440 (54) Araujo, J. B.; Brusseau, M. L. Assessing XMT-Measurement Variability of Air-Water  
441 Interfacial Areas in Natural Porous Media. *Water Resour Res* **2020**, *56* (1), 1–10.  
442 <https://doi.org/10.1029/2019WR025470>.

443 (55) Brusseau, M. L.; Araujo, J. B.; Narter, M.; Marble, J. C.; Bigler, M. Microtomographic  
444 Measurements of Total Air-Water Interfacial Areas for Soils. *Water Resour Res* **2024**,  
445 *60* (5). <https://doi.org/10.1029/2023WR036039>.

446 (56) Schaefer, C. E.; DiCarlo, D. A.; Blunt, M. J. Experimental Measurement of Air-Water  
447 Interfacial Area during Gravity Drainage and Secondary Imbibition in Porous Media.  
448 *Water Resour Res* **2000**, *36* (4), 885–890. <https://doi.org/10.1029/2000WR900007>.

449 (57) Brusseau, M. L.; Popovičová, J.; Silva, J. A. K. Characterizing Gas–Water Interfacial  
450 and Bulk-Water Partitioning for Gas-Phase Transport of Organic Contaminants in  
451 Unsaturated Porous Media. *Environ Sci Technol* **1997**, *31* (6), 1645–1649.  
452 <https://doi.org/10.1021/es960475j>.

453 (58) Araujo, J. B.; Mainhagu, J.; Brusseau, M. L. Measuring Air-Water Interfacial Area for  
454 Soils Using the Mass Balance Surfactant-Tracer Method. *Chemosphere* **2015**, *134*,  
455 199–202. <https://doi.org/10.1016/j.chemosphere.2015.04.035>.

456 (59) Chen, L.; Kibbey, T. C. G. Measurement of Air-Water Interfacial Area for Multiple  
457 Hysteretic Drainage Curves in an Unsaturated Fine Sand. *Langmuir* **2006**, *22* (16),  
458 6874–6880. <https://doi.org/10.1021/la053521e>.

459 (60) Leverett, M. C. Capillary Behavior in Porous Solids. *Transactions of the AIME* **1941**,  
460 142 (01), 152–169. <https://doi.org/10.2118/941152-G>.

461 (61) Morrow, N. R. Physics and Thermodynamics of Capillary Action in Porous Media. *Ind  
462 Eng Chem* **1970**, *62* (6), 32–56. <https://doi.org/10.1021/ie50726a006>.

463 (62) Peng, S.; Brusseau, M. L. Impact of Soil Texture on Air-Water Interfacial Areas in  
464 Unsaturated Sandy Porous Media. *Water Resour Res* **2005**, *41* (3), 5393–5399.  
465 <https://doi.org/10.1029/2004WR003233>.

466 (63) Brusseau, M. L. Determining Air-Water Interfacial Areas for the Retention and  
467 Transport of PFAS and Other Interfacially Active Solutes in Unsaturated Porous  
468 Media. *Science of the Total Environment* **2023**, *884* (December 2022), 163730.  
469 <https://doi.org/10.1016/j.scitotenv.2023.163730>.

470 (64) Zhang, W.; Guo, B. Anomalous Adsorption of PFAS at the Thin-Water-Film Air-Water  
471 Interface in Water-Unsaturated Porous Media. *Water Resour Res* **2024**, *60* (3).  
472 <https://doi.org/10.1029/2023WR035775>.

473 (65) Chen, S.; Guo, B. Pore-Scale Modeling of PFAS Transport in Water-Unsaturated  
474 Porous Media: Air–Water Interfacial Adsorption and Mass-Transfer Processes in Thin  
475 Water Films. *Water Resour Res* **2023**, *59* (8), 1–23.  
476 <https://doi.org/10.1029/2023WR034664>.

477 (66) Lenhart, J. J.; Saiers, J. E. Transport of Silica Colloids through Unsaturated Porous  
478 Media: Experimental Results and Model Comparisons. *Environ Sci Technol* **2002**, *36*  
479 (4), 769–777. <https://doi.org/10.1021/es0109949>.

480 (67) Saiers, J. E.; Lenhart, J. J. Colloid Mobilization and Transport within Unsaturated  
481 Porous Media under Transient-Flow Conditions. *Water Resour Res* **2003**, 39 (1).  
482 <https://doi.org/10.1029/2002WR001370>.

483 (68) Šimůnek, J.; He, C.; Pang, L.; Bradford, S. A. Colloid-Facilitated Solute Transport in  
484 Varily Saturated Porous Media. *Vadose Zone Journal* **2006**, 5 (3), 1035.  
485 <https://doi.org/10.2136/vzj2005.0151>.

486 (69) Bradford, S. A.; Torkzaban, S. Colloid Transport and Retention in Unsaturated Porous  
487 Media: A Review of Interface-, Collector-, and Pore-Scale Processes and Models.  
488 *Vadose Zone Journal* **2008**, 7 (2), 667–681. <https://doi.org/10.2136/vzj2007.0092>.

489 (70) Pope, G. A.; Nelson, R. C. A Chemical Flooding Compositional Simulator. *Society of*  
490 *Petroleum Engineers Journal* **1978**, 18 (05), 339–354. <https://doi.org/10.2118/6725-PA>.

492 (71) Delshad, M., Pope, G.A. and Sepehrnoori, K. UTCHEM Version 9.0 Technical  
493 Documentation. Center for Petroleum and Geosystems Engineering, The University  
494 of Texas at Austin, Austin, Texas, 78751. 2000.

495 (72) Pennell, K. D.; Abriola, L. M.; Weber, W. J. Surfactant-Enhanced Solubilization of  
496 Residual Dodecane in Soil Columns. 1. Experimental Investigation. *Environ Sci*  
497 *Technol* **1993**, 27 (12), 2332–2340. <https://doi.org/10.1021/es00048a005>.

498 (73) Delshad, M.; Pope, G. A.; Sepehrnoori, K. A Compositional Simulator for Modeling  
499 Surfactant Enhanced Aquifer Remediation, 1 Formulation. *J Contam Hydrol* **1996**, 23  
500 (4), 303–327. [https://doi.org/10.1016/0169-7722\(95\)00106-9](https://doi.org/10.1016/0169-7722(95)00106-9).

501 (74) Smith, J. E.; Gillham, R. W. The Effect of Concentration-dependent Surface Tension  
502 on the Flow of Water and Transport of Dissolved Organic Compounds: A Pressure  
503 Head-based Formulation and Numerical Model. *Water Resour Res* **1994**, 30 (2), 343–  
504 354. <https://doi.org/10.1029/93WR02745>.

505 (75) Henry, E. J.; Smith, J. E. Surfactant-Induced Flow Phenomena in the Vadose Zone: A  
506 Review of Data and Numerical Modeling. *Vadose Zone Journal* **2003**, 2 (2), 154–167.  
507 <https://doi.org/10.2113/2.2.154>.

508 (76) Costanza-Robinson, M. S.; Henry, E. J. Surfactant-Induced Flow Compromises  
509 Determination of Air-Water Interfacial Areas by Surfactant Miscible-Displacement.  
510 *Chemosphere* **2017**, 171, 275–283.  
511 <https://doi.org/10.1016/j.chemosphere.2016.12.072>.

512 (77) Brusseau, M. L.; Van Glubt, S. The Influence of Surfactant and Solution Composition  
513 on PFAS Adsorption at Fluid-Fluid Interfaces. *Water Res* **2019**, *161*, 17–26.  
514 <https://doi.org/10.1016/j.watres.2019.05.095>.

515 (78) Silva, J. A. K.; Martin, W. A.; Johnson, J. L.; McCray, J. E. Evaluating Air-Water and  
516 NAPL-Water Interfacial Adsorption and Retention of Perfluorocarboxylic Acids within  
517 the Vadose Zone. *J Contam Hydrol* **2019**, *223* (March), 103472.  
518 <https://doi.org/10.1016/j.jconhyd.2019.03.004>.

519 (79) Le, S. T.; Gao, Y.; Kibbey, T. C. G.; Glamore, W. C.; O’Carroll, D. M. A New Framework  
520 for Modeling the Effect of Salt on Interfacial Adsorption of PFAS in Environmental  
521 Systems. *Science of the Total Environment* **2021**, *796*, 148893.  
522 <https://doi.org/10.1016/j.scitotenv.2021.148893>.

523 (80) Gao, Y.; Le, S. T.; Kibbey, T. C. G.; Glamore, W.; O’Carroll, D. M. A Fundamental Model  
524 for Calculating Interfacial Adsorption of Complex Ionic and Nonionic PFAS Mixtures  
525 in the Presence of Mixed Salts. *Environ Sci Process Impacts* **2023**.  
526 <https://doi.org/10.1039/d2em00466f>.

527 (81) Guo, B.; Saleem, H.; Brusseau, M. L. Predicting Interfacial Tension and Adsorption at  
528 Fluid–Fluid Interfaces for Mixtures of PFAS and/or Hydrocarbon Surfactants. *Environ  
529 Sci Technol* **2023**, *57* (21), 8044–8052. <https://doi.org/10.1021/acs.est.2c08601>.

530 (82) Costanza, J.; Arshadi, M.; Abriola, L. M.; Pennell, K. D. Accumulation of PFOA and  
531 PFOS at the Air–Water Interface. *Environ Sci Technol Lett* **2019**, *6* (8), 487–491.  
532 <https://doi.org/10.1021/acs.estlett.9b00355>.

533 (83) Silva, J. A. K.; Martin, W. A.; McCray, J. E. Air-Water Interfacial Adsorption Coefficients  
534 for PFAS When Present as a Multi-Component Mixture. *J Contam Hydrol* **2021**, *236*  
535 (October 2020), 103731. <https://doi.org/10.1016/j.jconhyd.2020.103731>.

536 (84) Huang, D.; Saleem, H.; Guo, B.; Brusseau, M. L. The Impact of Multiple-Component  
537 PFAS Solutions on Fluid-Fluid Interfacial Adsorption and Transport of PFOS in  
538 Unsaturated Porous Media. *Science of The Total Environment* **2022**, *806*, 150595.  
539 <https://doi.org/10.1016/j.scitotenv.2021.150595>.

540 (85) Anderson, R. H.; Field, J. B.; DieffenbachCarle, H.; Elsharnouby, O.; Krebs, R. K.  
541 Assessment of PFAS in Collocated Soil and Porewater Samples at an AFFF-Impacted  
542 Source Zone: Field-Scale Validation of Suction Lysimeters. *Chemosphere* **2022**, *308*  
543 (P1), 136247. <https://doi.org/10.1016/j.chemosphere.2022.136247>.

544 (86) Nickerson, A.; Rodowa, A. E.; Adamson, D. T.; Field, J. A.; Kulkarni, P. R.; Kornuc, J. J.;  
545 Higgins, C. P. Spatial Trends of Anionic, Zwitterionic, and Cationic PFASs at an AFFF-

546                    Impacted Site. *Environ Sci Technol* **2021**, 55 (1), 313–323.  
547                    <https://doi.org/10.1021/acs.est.0c04473>.

548 (87) Adamson, D. T.; Nickerson, A.; Kulkarni, P. R.; Higgins, C. P.; Popovic, J.; Field, J.;  
549 Rodowa, A.; Newell, C.; Deblanc, P.; Kornuc, J. J. Mass-Based, Field-Scale  
550 Demonstration of PFAS Retention within AFFF-Associated Source Areas. *Environ Sci  
551 Technol* **2020**, 54 (24), 15768–15777. <https://doi.org/10.1021/acs.est.0c04472>.

552 (88) Ruyle, B. J.; Thackray, C. P.; McCord, J. P.; Strynar, M. J.; Mauge-Lewis, K. A.; Fenton,  
553 S. E.; Sunderland, E. M. Reconstructing the Composition of Per- And Polyfluoroalkyl  
554 Substances in Contemporary Aqueous Film-Forming Foams. *Environ Sci Technol Lett*  
555 **2021**, 8 (1), 59–65. <https://doi.org/10.1021/acs.estlett.0c00798>.

556 (89) Field, J. A.; Seow, J. Properties, Occurrence, and Fate of Fluorotelomer Sulfonates.  
557 *Crit Rev Environ Sci Technol* **2017**, 47 (8), 643–691.  
558 <https://doi.org/10.1080/10643389.2017.1326276>.

559 (90) Liu, M.; Munoz, G.; Vo Duy, S.; Sauvé, S.; Liu, J. Per- and Polyfluoroalkyl Substances in  
560 Contaminated Soil and Groundwater at Airports: A Canadian Case Study. *Environ Sci  
561 Technol* **2022**, 56 (2), 885–895. <https://doi.org/10.1021/acs.est.1c04798>.

562 (91) Baduel, C.; Mueller, J. F.; Rotander, A.; Corfield, J.; Gomez-Ramos, M. J. Discovery of  
563 Novel Per- and Polyfluoroalkyl Substances (PFASs) at a Fire Fighting Training Ground  
564 and Preliminary Investigation of Their Fate and Mobility. *Chemosphere* **2017**, 185,  
565 1030–1038. <https://doi.org/10.1016/j.chemosphere.2017.06.096>.

566 (92) Schumacher, B. A.; Zimmerman, J. H.; Williams, A. C.; Lutes, C. C.; Holton, C. W.;  
567 Escobar, E.; Hayes, H.; Warrier, R. Distribution of Select Per- and Polyfluoroalkyl  
568 Substances at a Chemical Manufacturing Plant. *J Hazard Mater* **2024**, 464, 133025.  
569 <https://doi.org/10.1016/j.jhazmat.2023.133025>.

570 (93) Liu, J.; Mejia Avendaño, S. Microbial Degradation of Polyfluoroalkyl Chemicals in the  
571 Environment: A Review. *Environ Int* **2013**, 61, 98–114.  
572 <https://doi.org/10.1016/j.envint.2013.08.022>.

573 (94) Choi, Y. J.; Helbling, D. E.; Liu, J.; Olivares, C. I.; Higgins, C. P. Microbial  
574 Biotransformation of Aqueous Film-Forming Foam Derived Polyfluoroalkyl  
575 Substances. *Science of The Total Environment* **2022**, 824, 153711.  
576 <https://doi.org/10.1016/j.scitotenv.2022.153711>.

577 (95) Ruyle, B. J.; Thackray, C. P.; Butt, C. M.; Leblanc, D. R.; Tokranov, A. K.; Vecitis, C. D.;  
578 Sunderland, E. M. Centurial Persistence of Forever Chemicals at Military Fire Training

579 Sites. *Environ Sci Technol* **2023**, 57(21), 8096–8106.  
580 <https://doi.org/10.1021/acs.est.3c00675>.

581 (96) Brusseau, M. L.; Guo, B. Vapor-Phase Transport of Per and Polyfluoroalkyl  
582 Substances: Processes, Modeling, and Implications. *Science of the Total  
583 Environment* **2024**.

584 (97) Abusallout, I.; Holton, C.; Wang, J.; Hanigan, D. Henry's Law Constants of 15 per- and  
585 Polyfluoroalkyl Substances Determined by Static Headspace Analysis. *Journal of  
586 Hazardous Materials Letters* **2022**, 3, 100070.  
587 <https://doi.org/10.1016/j.hazl.2022.100070>.

588 (98) Vahedian, F.; Silva, J. A. K.; Šimůnek, J.; McCray, J. E. Influence of Tension-Driven  
589 Flow on the Transport of AFFF in Unsaturated Media. *ACS ES&T Water* **2024**, 4 (2),  
590 564–574. <https://doi.org/10.1021/acsestwater.3c00611>.

591 (99) Silva, J. A. K.; Martin, W. A.; McCray, J. E. Air-Water Interfacial Adsorption Coefficients  
592 for PFAS When Present as a Multi-Component Mixture. *J Contam Hydrol* **2020**, No.  
593 November 2019, 103731. <https://doi.org/10.1016/j.jconhyd.2020.103731>.

594 (100) Guo-Xi, Z.; Bu-Yao, Z.; Ya-Ping, Z.; Li, S. The Surface Adsorption and Micelle  
595 Formation of the Mixed Aqueous Solutions of Fluorocarbon and Hydrocarbon  
596 Surfactants: II. Sodium Perfluorooctanoate-Sodium Decylsulfate System. *Acta Chim  
597 Sin* **1984**, 2 (2), 111–118. <https://doi.org/10.1002/cjoc.19840020205>.

598 (101) Schaefer, C. E.; Culina, V.; Nguyen, D.; Field, J. A. Uptake of Poly- and Perfluoroalkyl  
599 Substances at the Air-Water Interface. *Environ Sci Technol* **2019**, 53, 12442–12448.  
600 <https://doi.org/10.1021/acs.est.9b04008>.

601 (102) Vecitis, C. D.; Park, H.; Cheng, J.; Mader, B. T.; Hoffmann, M. R. Enhancement of  
602 Perfluorooctanoate and Perfluorooctanesulfonate Activity at Acoustic Cavitation  
603 Bubble Interfaces. *Journal of Physical Chemistry C* **2008**, 112 (43), 16850–16857.  
604 <https://doi.org/10.1021/jp804050p>.

605 (103) Lyu, X.; Li, Z.; Wang, D.; Zhang, Q.; Gao, B.; Sun, Y.; Wu, J. Transport of  
606 Perfluorooctanoic Acid in Unsaturated Porous Media Mediated by SDBS. *J Hydrol  
607 (Amst)* **2022**, 607 (January), 127479. <https://doi.org/10.1016/j.jhydrol.2022.127479>.

608 (104) Abraham, J. E. F.; Mumford, K. G.; Patch, D. J.; Weber, K. P. Retention of PFOS and  
609 PFOA Mixtures by Trapped Gas Bubbles in Porous Media. **2022**.  
610 <https://doi.org/10.1021/acs.est.2c00882>.

611 (105) Liao, S.; Arshadi, M.; Woodcock, M. J.; Saleeba, Z. S. S. L.; Pinchbeck, D.; Liu, C.;  
612 Cápiro, N. L.; Abriola, L. M.; Pennell, K. D. Influence of Residual Nonaqueous-Phase  
613 Liquids (NAPLs) on the Transport and Retention of Perfluoroalkyl Substances.  
614 *Environ Sci Technol* **2022**, 56 (12), 7976–7985.  
615 <https://doi.org/10.1021/acs.est.2c00858>.

616 (106) Ji, Y.; Yan, N.; Brusseau, M. L.; Guo, B.; Zheng, X.; Dai, M.; Liu, H.; Li, X. Impact of a  
617 Hydrocarbon Surfactant on the Retention and Transport of Perfluorooctanoic Acid in  
618 Saturated and Unsaturated Porous Media. *Environ Sci Technol* **2021**, 55 (15), 10480–  
619 10490. <https://doi.org/10.1021/acs.est.1c01919>.

620 (107) Arshadi, M.; Garza-Rubalcava, U.; Guedes, A.; Cápiro, N. L.; Pennell, K. D.; Christ, J.;  
621 Abriola, L. M. Modeling 1-D Aqueous Film Forming Foam Transport through the  
622 Vadose Zone under Realistic Site and Release Conditions. *Science of The Total  
623 Environment* **2024**, 919, 170566. <https://doi.org/10.1016/j.scitotenv.2024.170566>.

624 (108) Kemball; Rideal; Guggenheim. Thermodynamics of Monolayers. **1948**, No. 948, 399–  
625 407.

626 (109) Broughton, D. B. Adsorption Isotherms for Binary Gas Mixtures. *Ind Eng Chem* **1948**,  
627 40 (8), 1506–1508. <https://doi.org/10.1021/ie50464a036>.

628 (110) Levanr, M. D.; Vermeulen, T. Binary Langmuir and Freundlich Isotherms for Ideal  
629 Adsorbed Solutions. **1981**, 948 (1948), 3247–3250.

630 (111) Frey, D. D.; Rodrigues, A. E. Explicit Calculation of Multicomponent Equilibria for  
631 Ideal Adsorbed Solutions. *AIChE Journal* **1994**, 40 (1), 182–186.  
632 <https://doi.org/10.1002/aic.690400121>.

633 (112) Celia, M. A.; Bouloutas, E. T.; Zarba, R. L. A General Mass-Conservative Numerical  
634 Solution for the Unsaturated Flow Equation. *Water Resour Res* **1990**, 26 (7), 1483–  
635 1496. <https://doi.org/10.1029/WR026i007p01483>.

636 (113) Pinder, G.; Celia, M. *Subsurface Hydrology*; John Wiley & Sons, 2006.

637